Inorganica Chimica Acta 366 (2011) 357–365

Contents lists available at ScienceDirect

Inorganica Chimica Acta

journal homepage: www.elsevier.com/locate/ica

The replacement of chlorides by cytosines in copper(II) complexes containing guanidine derivatives

Atittaya Meenongwa, Unchulee Chaveerach *, Khatcharin Siriwong

Department of Chemistry and Center of Excellence for Innovation in Chemistry, Faculty of Science, Khon Kaen University, Khon Kaen 40002, Thailand

ARTICLE INFO

Article history:
Received 15 July 2010
Received in revised form 10 September 2010
Accepted 18 November 2010
Available online 1 December 2010

Keywords:
Copper(II)
Cytosine binding
Amidino-*O*-alkylurea
Spectroscopic analysis
Theoretical calculation

ABSTRACT

Two copper(II) chloride complexes of amidino-*O*-methylurea (L^1), $[Cu(L^1)Cl_2]$ (**1**), and (*N*-benzyl)-amidino-*O*-methylurea (L^2), $[Cu(L^2)Cl_2]$ (**2**), were prepared and characterized by elemental analysis, infrared, diffuse reflectance, electron spin resonance and electrospray ionization mass spectra. Their cytosine binding abilities has been studied and found that two cytosine molecules are able to coordinate with the copper centers by replacing the chloride ligands to yield the bifunctional binding adducts $[Cu(L^1)(cyt)_2]Cl_2$ (**1c**) and $[Cu(L^2)(cyt)_2]Cl_2$ (**2c**), respectively. The shift of the C=O band of cytosine in both cytosine-bound products to higher energy suggested that the N(3)–cytosine atom coordinates to the copper center. The large blue shifts of the d–d absorbance maxima and the nine superhyperfine splitting from the CuN_4 chromophore were also observed in their electronic and EPR spectra. Their thermal decompositions have also supported the interaction of cytosine with complexes **1** and **2**. Density functional calculations have also been performed and revealed that square planar coordination geometry is more stable for both **1c** and **2c**. The binding energy of **1c** is found to be ~20% lower than that of **2c**, indicative of the higher binding potential of **1c**.

1. Introduction

The success of an anticancer drug cisplatin, $[PtCl_2(NH_3)_2]$, has led to the development in a large number of metal-based chemotherapy drugs. Cisplatin is a small molecule containing a square planar PtN_2Cl_2 unit. Its biological activity is believed that one of the chloride ligands is slowly displaced by an aqua ligand yielding $[PtCl(H_2O)(NH_3)_2]^+$ which is subsequently reacted with a basic site in DNA. Finally, cross-linking of the two DNA bases, particularly guanines, takes place by means of displacement of the remaining chloride ligand [1,2], thereby interfering with mitosis and then undergoing apoptosis. Hence, the lability of two chlorides is of importance in the anticancer activity. Although cisplatin offers a good result in treatment of cancer patients, several side-effects such as nephrotoxicity, neurotoxicity, nausea and vomiting are found [3]. As a result, there is a need for searching new agents which do not exhibit cross-resistance and which are less toxic.

Cisplatin analogs containing the PtN_2Cl_2 chromophore have been synthesized by several research groups [4–8]. However, coordination compounds of other transition metals, such as palladium(II), gold(III), ruthenium(II), copper(II) and etc., have also been studied in terms of the interactions with nucleic acids and their cytotoxicity. Particularly, copper(II) ion, which plays an important role in all living systems as an essential trace element [9], has currently received intense interest prior to its structural diversity, redox property and DNA cleaving ability. For example, a series of copper(II) compounds containing *N*,*N*-bidentate benzimidazole derivatives with the CuN_2Cl_2 chromophore have been prepared and showed their biological activities toward cancer cell lines [10]. Moreover, three CuN_2Cl_2 complexes with guanidinium/ammonium groups were synthesized and investigated their cleavage efficiency [11]. These activities have guided us to prepare copper(II) complexes containing a CuN_2Cl_2 chromophore analog to cisplatin and then to study their interactions with DNA nucleobases. Several studies have mainly focused on the direct interaction of metal salts, where M = Cu, Rh, Cd, Mn or Co, with the cytosine nucleobase and its derivative 1-methylcytosine [12–19], but not the direct nucleobase replacement of the anionic ligands on metal complexes like the cisplatin system. However, Reedijk and coworkers have studied on interactions of the octahedral ruthenium(II) complexes [*cis*-$Ru(bpy)_2Cl_2$] [20] and [α-$Ru(azpy)_2(NO_3)_2$] [21] (bpy = 2,2′-bipyridine and azpy = 2-(phenylazo)pyridine) with 9-ethylguanine, 9-methylhypoxanthine and guanosine, which replace only one of the two anionic ligands to yield the monofunctional binding adducts.

Towards achieving our goal of finding a new choice of metal complexes based upon a cheaper alternative copper(II) ion showing an efficient binding potential to nucleobase, we firstly studied on the interaction of the two copper(II) chloride complexes,

* Corresponding author. Tel.: +66 43 202222x12243; fax: +66 43 202373.
E-mail address: sunchul@kku.ac.th (U. Chaveerach).

0020-1693/$ - see front matter © 2010 Elsevier B.V. All rights reserved.
doi:10.1016/j.ica.2010.11.030

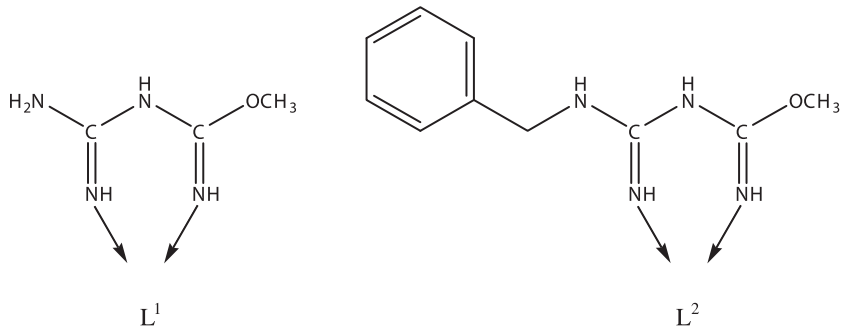

Scheme 1. Ligands in the present work. L^1 = amidino-*O*-methylurea and L^2 = (*N*-methylphenyl)-amindino-*O*-methylurea.

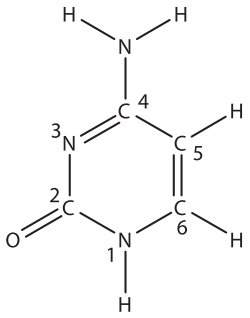

Scheme 2. Cytosine molecule with atomic numberings.

$[Cu(L^1)Cl_2]$ (**1**) and $[Cu(L^2)Cl_2]$ (**2**), where L^1 = amidino-*O*-methylurea and L^2 = (*N*-benzyl)-amidino-*O*-methylurea (Scheme 1), toward cytosine (cyt) molecules (Scheme 2). In 2003, the copper(II) chloride complex consisting of two L^2 ligands, $[Cu(L^2)_2]Cl_2$, has been structurally studied and reported [22] that the copper(II) center are coordinated by two symmetry-related *N*,*N*-bidentate L^2 ligands in a *trans* configuration to give a square planar geometry. In the present work, compounds **1** and **2** contain only a single molecule of L^1 and L^2 ligands, respectively, which only differ in the *N*-substitution sidearm groups, NH_2 for **1** and NH_2CH_2Ph for **2** (Scheme 1). This will give us an opportunity to examine the pendent-arm effect on their cytosine-binding abilities. Besides, other advantages of this complex system are that (i) complexes **1** and **2** are similar to cisplatin in that they contain the same MN_2Cl_2 (M = Cu or Pt) chromophore; (ii) the L^1 and L^2 ligands are an *N*,*N*-bidentate ligand which will chelate to a copper center and give a more stable complex; (iii) this ligand system also results a compound in *cis*-isomer, just like cisplatin; and (iv) hence, one site of complexes **1** and **2** is blocked by the L^1 and L^2 ligands and another site is situated by two labile groups (Cl^-) which will be easily replaced by nucleobases such as cytosine. It was found that the predominant metal binding site of cytosine nucleobase is the nitrogen atom N(3) (Scheme 2) [11,12,14,15,17,23,24]. In addition, the secondary interaction between copper and the O(2) exocyclic carbonyl group of cytosine also exists in a few cases [16,25,26].

Herein, our attempts were to prepare two copper(II) complexes of $[Cu(L^1)Cl_2]$ (**1**) and $[Cu(L^2)Cl_2]$ (**2**) and investigate their interactions toward cytosine nucleobases. Spectroscopic methods (infrared, electrospray ionization mass, diffuse reflectance and electron spin resonance), elemental analysis and thermogravimetric analysis were utilized to give some evidences for the cytosine replacement by the two chlorides in both compounds. Additionally, density functional calculations for the cytosine-bound complexes have been carried out to obtain the binding energies and predict theoretically their coordination geometries.

2. Experimental

2.1. Materials and methods

Copper(II) chloride dihydrate, cyanoguanidine and cytosine were purchased from Sigma–Aldrich Chemical Company Ltd. and used without further purification. The elemental analysis was determined using a Perkin–Elmer PE-2400II CHNS/O elemental analyzer. The infrared spectra were obtained in the range 4000–400 cm^{-1} as KBr pressed pellets on a Perkin–Elmer spectrum one FT-IR spectrophotometer. Diffuse reflectance spectra were obtained on a Shimadzu 3101 UV–Vis–NIR scanning spectrophotometer. Positive electrospray ionization (ESI+) mass spectral measurements were undertaken using a Q-TOF mass spectrometer. Thermogravimetric curves were obtained on a Perkin–Elmer Pyris Diamond TG/DTA thermal analyzer with a heating rate of 5 °C min^{-1} from 30 to 1000 °C under 100 mL min^{-1} N_2 flow. Electron spin resonance spectra in the frozen DMSO solution at 77 K were recorded by a RE-2X electron spin resonance spectrometer operating at ν = 9.16 GHz (X-band).

2.2. Copper(II) complex preparations

Copper(II) complexes $[Cu(L^1)Cl_2]$ (**1**) and $[Cu(L^2)Cl_2]$ (**2**) were prepared by the slightly modified procedure as previously reported [27]. A 1:1 molar ratio of $CuCl_2{\cdot}2H_2O$ (0.3410 g; 2 mmol) and cyanoguanidine for **1** (0.1682 g; 2 mmol) or (*N*-benzyl)-cyanoguanidine for **2** (0.3480 g; 2 mmol) was used instead. The preparation reactions were shown below.

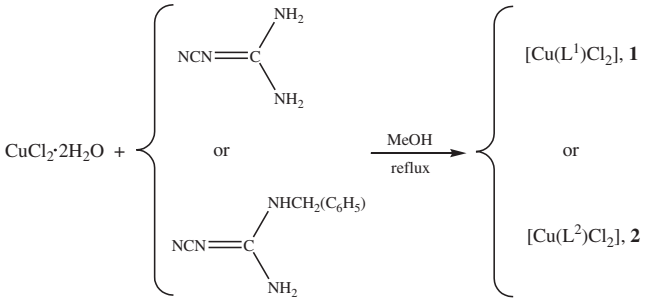

2.2.1. $[Cu(L^1)Cl_2]$, **1**

Yield: 0.4920 g; 1.96 mmol; 98.2%. M.p. (°C): 228.4–229.2. *Anal.* Calc. for $C_3H_8N_4OCuCl_2$: C, 14.37; H, 3.19; N, 22.36. Found: C, 14.02; H, 3.14; N, 22.63%. IR (KBr/cm^{-1}): 3373s, br; 3343s, br; 3259s, br; 3180s, br; 1692s; 1656s; 1547s; 1508m; 1430m; 1343m; 1197m; 1165m; 1117w; 948w; 760m; 732m; 688w;

647w; 568w; 518m; 453w. Diffuse reflectance (λ_{max}/cm^{-1}): 15 049. ESI+ mass spec (*m/z*): 179 $[Cu(L^1)-H^+]^+$; 117 $[(L^1)H]^+$.

*2.2.2. $[Cu(L^2)Cl_2]$, **2***

Yield: 0.4147 g; 1.22 mmol; 60.9%. M.p. (°C): 209.9–210.3. *Anal.* Calc. for $C_{10}H_{14}N_4OCuCl_2$: C, 35.24; H, 4.11; N, 16.45. Found: C, 35.40; H, 4.25; N, 16.73%. IR (KBr/cm^{-1}): 3375m, br; 3301s, br; 3225m, br; 3144m, br; 2961w; 1677s; 1556s; 1525m; 1442m; 1385m; 1356m; 1326m; 1226m; 1211m; 1169m; 1144m; 1089w; 1055w; 930w; 897w; 774w; 734m; 712m; 696m; 610w; 535w. Diffuse reflectance (λ_{max}/cm^{-1}): 16 176. ESI+ mass spec (*m/z*): 268 $[Cu(L^2)-H^+]^+$; 207 $[(L^2)H]^+$.

2.3. Cytosine binding to copper(II) complexes

Cytosine (0.0888 g; 0.8 mmol) was added into 25 mL of the warm ethanol–water (1:2 v/v) solution of complex **1** (0.1002 g; 0.4 mmol) or complex **2** (0.1362 g; 0.4 mmol). The dark blue solution was stirred under reflux condition for 24 h. A pink or purple solid, respectively, was obtained by solvent reduction under vacuum. The binding reactions were shown below.

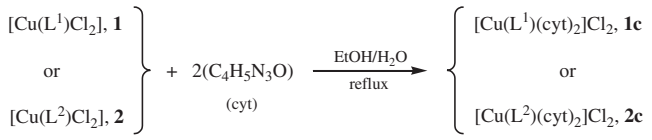

*2.3.1. $[Cu(L^1)(cyt)_2)]Cl_2$, **1c***

Yield: 0.1705 g; 0.36 mmol; 90.2%. M.p. (°C): 181.2–184.2. *Anal.* Calc. for $C_{11}H_{18}N_{10}O_3CuCl_2$: C, 27.94; H, 3.81; N, 29.63. Found: C, 27.98; H, 3.82; N, 29.63%. IR (KBr/cm^{-1}): 3370s, br; 3305s, br; 3193s, br; 2996s; 1746m; 16721s; 1614s; 1497m; 1447m; 1370m; 1298w; 1236m; 1218m; 1146w; 1126w; 1012w; 947w; 843w; 807m; 784m; 760m; 599m; 579w; 547w; 431w. Diffuse reflectance (λ_{max}/cm^{-1}): 19 327. ESI+ mass spec (*m/z*): 400 $[Cu(L^1)(cyt)_2-H^+]^+$; 289 $[Cu(L^1)(cyt)-H^+]^+$; 118 $[(L^1)+2H^+]$; 112 $[(cyt)+H^+]$. TGA Found (calc): $[Cu(cyt)]Cl^+$ (50–450 °C) 45.2 (44.4); $CuCl^+$ (450–1100 °C) 22.4 (20.9).

*2.3.2. $[Cu(L^2)(cyt)_2)]Cl_2$, **2c***

Yield: 0.1922 g; 0.34 mmol; 85.4%. M.p. (°C): 186.8–187.4. *Anal.* Calc. for $C_{18}H_{24}N_{10}O_3CuCl_2$: C, 38.40; H, 4.27; N, 24.89. Found: C, 38.49; H, 4.25; N, 24.88%. IR (KBr/cm^{-1}): 3294s, br; 3220s; 3120s, br; 2974s; 1738m; 1667s; 1591m; 1496m; 1457m; 1365w; 1297w; 1219m; 1156w; 1030w; 952w; 904w; 800m; 780m; 760m; 731m; 700m; 600m; 578m; 544w; 475w. Diffuse reflectance (λ_{max}/cm^{-1}): 19 153. ESI+ mass spec (*m/z*): 490 $[Cu(L^2)(cyt)_2-H^+]^+$; 379 $[Cu(L^2)(cyt)-H^+]^+$; 268 $[Cu(L^2)-H^+]^+$; 207 $[(L^2)H]^+$. TGA Found (calc): $[Cu(L^2)(cyt)_2]^{2+}$ (60–230 °C) 87.9 (87.4); $[Cu(cyt)]^{2+}$ (230–425 °C) 31.7 (31.0).

2.4. Computational details

In order to investigate the binding competence between cytosine bases and the two copper(II) complexes (**1** and **2**) and to predict the geometry of cytosine-bound complexes (**1c** and **2c**), the first principle density functional (DF) calculations were used. The structures of cytosine, $[Cu(L^1)]^{2+}$, $[Cu(L^2)]^{2+}$, $[Cu(L^1)(cyt)_2]^{2+}$ and $[Cu(L^2)(cyt)_2]^{2+}$ were optimized without restriction using Dmol^3 module of Material Studio 4.3 package [28] at the National Nanotechnology Center, Thailand. The numerical basis sets of double zeta quality plus polarization functions (DNP) were employed in all calculations to describe the valence orbitals. The density functional semi-core pseudo-potentials (DSPP) [29] were also utilized to treat core electrons. The exchange–correlation contribution to the total electronic energy was treated in a generalized-gradient approximation (GGA-PW91) function. It was previously reported that these functions have been successfully used to predict geometry and energy for the anticancer drug oxaliplatin [30,31]. The binding energy ($\Delta E_{binding}$) including relaxation can be expressed as

$$\Delta E_{binding} = E_{Cu(L)(cyt)_2} - (E_{Cu(L)} + 2E_{cyt})$$

where $E_{Cu(L)(cyt)_2}$, $E_{Cu(L)}$ and E_{cyt} are the zero-point corrected energies of the optimized structure for $[Cu(L)(cyt)_2]^{2+}$, $[Cu(L)]^{2+}$, and cytosine, respectively. L is either the ligand L^1 or L^2.

3. Results and discussion

3.1. General aspects

The pale blue $[Cu(L^1)Cl_2]$ (**1**) and deep blue $[Cu(L^2)Cl_2]$ (**2**) complexes were generated in a good yield by methanolysis reaction of cyanoguanidine and (*N*-benzyl)-cyanoguanidine, respectively, in the presence of copper(II) chloride in a 1:1 molar ratio. Their elemental analyses were in agreement with the desired compounds.

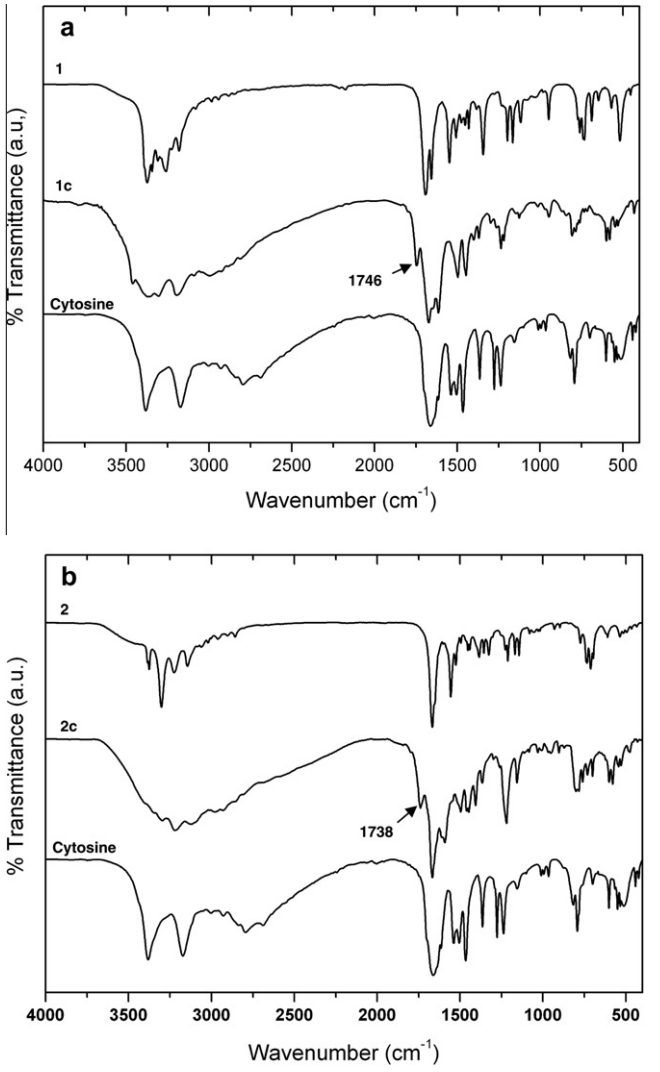

Fig. 1. Overlayered FT-IR spectra of the free complexes **1** and **2** (top), the bound complexes **1c** and **2c** (middle) and cytosine (bottom).

The molecular ion peak of the cationic species, $[Cu(L^1)-H^+]^+$ for **1** and $[Cu(L^2)-H^+]^+$ for **2**, was appeared at m/z = 179 and 268, respectively, in their ESI+ mass spectra. Additionally, the protonated ligands were observed at m/z = 117 for $[(L^1)H]^+$ and 207 for $[(L^2)H]^+$. Melting points were observed in the narrow temperature range of 228.4–229.2 for **1** and 209.9–210.3 °C for **2**.

Subsequently, the binding experiments were carried out in a 1:2 molar ratio of the obtained complexes and cytosine nucleobases. Colors of the resulting products were changed to pink (**1c**) and purple (**2c**). Their melting properties were significantly changed to 181.2–184.2 °C for **1c** and 186.8–187.4 °C for **2c**. These modifications preliminarily point out that environment on copper(II) centers of the bound compounds totally differ from that of the free compounds. Thus it is suggested that the interaction between compounds **1** or **2** and cytosine bases has taken place. To gain further evidences on the cytosine binding ability of **1** and **2**, various spectroscopic methods (infrared, mass, diffuse reflectance, electron spin resonance), thermal analysis and density functional calculations were undertaken and deeply described in the following topics.

3.2. Analysis of infrared spectra

Vibrational spectrophotometry is a basis method to determine the functional groups of compounds. Herein, it can be used to monitor the interaction between the starting copper(II) complexes and cytosine nucleobases. Infrared spectra of the free complexes (**1** and **2**), cytosine and the bound complexes (**1c** and **2c**) are illustrated in Fig. 1. Band assignments are listed in Table 1.

Infrared spectra of **1c** and **2c** revealed the presence of all functional groups from both cytosine and the corresponding free complexes. The strong and broad infrared absorption bands in the range 3370–3120 cm^{-1} are assigned to asymmetric and symmetric NH_2 stretching vibrations of both cytosine and the free complexes. The broadening CH stretching bands of complexes **1c** and **2c** were also observed in the range of 2996–2974 cm^{-1}. The N–H bending vibrations also appeared in the range of 1672–1447 cm^{-1}. The bands assigned to C=C and C=N stretching vibrations were shifted from 1614–1539 cm^{-1} for the free cytosine to higher frequency at 1672–1591 cm^{-1} for the bound complexes since the conjugated π-electrons in the cytosine ring were redistributed. This evidence preliminarily confirms the coordination of the N(3) cytosine to the copper(II) center of **1** and **2** [32]. In addition, the bands related to ν-ring and ν(C–N) single bonded stretching frequencies were found in their infrared spectra in the lower frequency than 1500 cm^{-1}.

It is noticed in the region of 1750–1730 cm^{-1} that the additional new peak at 1746 and 1738 cm^{-1} corresponding to the C=O stretching vibration of cytosine was observed in compounds **1c** and **2c**, respectively. The C=O band of the free cytosine at ~1665 cm^{-1} was shifted to higher frequency in both compounds, thus eliminating the exocyclic O(2) coordination of cytosine. The shift of infrared bands in the complexes is therefore a more and strong evidence to suggest that cytosine molecules coordinate to the copper center of **1** and **2**.

Table 1
Assignment of infrared vibrational modes for cytosine, the free complexes (**1** and **2**) and the bound complexes (**1c** and **2c**)

Cytosine	Wave number (cm^{-1})[a]				Assignment
	Free complex		Bound complex		
	1	**2**	**1c**	**2c**	
3382s, br	3373s, br	3375m, br	3370s, br	3294s, br	ν_{as}(NH)
	3343s, br	3301s, br	3305s, br		ν_{as}(NH)
	3259s, br	3225m, br		3220s	ν_s(NH)
3172s, br	3180s, br	3144m, br	3193s, br	3120s, br	ν_s(NH)
2927s	2984w	2961w	2996s	2974s	ν (CH)
1665s			**1746m**	**1738m**	ν(**C**=O)
	1692s	1677s	1672s	1667s	ν(C=C), ν(C=N), $\delta(NH_2)$
1614s, sh	1656s		1614s	1591m	ν(C=C), ν(C=N), $\delta(NH_2)$
1539s	1547s	1556s			ν(ring), ν(C=N), $\delta(NH_2)$
1504m	1508m	1525m	1497m	1496m	ν(ring), ν(C–NH_2), $\delta(NH_2)$
1466m	1430m	1442m	1447m	1457m	ν(ring), ν(C–N), $\delta(NH_2)$, δ(CH)
1364m	1343m	1385m	1370m	1365w	ν(ring), δ(CH)
		1356m			ν(ring), δ(CH)
1277m		1326m	1298w	1297w	ν(ring), δ(CH)
1237m			1236m		ν(ring), δ(CH)
		1226m		1219m	ν(ring), δ(CH)
	1197m	1211m	1218m		ν(ring), $\rho(NH_2)$, ν(C–O)
	1165m	1169m			ν(ring), $\rho(NH_2)$, ν(C–O)
1155w		1144m	1146w	1156w	ν(ring), $\rho(NH_2)$, ν(C–O)
	1117w	1089w	1126w		ν(ring), $\rho(NH_2)$, ν(C–O)
1010w		1055w	1012w	1030w	ν(ring), $\rho(NH_2)$
994w					ν(ring), $\rho(NH_2)$
965w					ν(ring), $\rho(NH_2)$
	948m	930w	947w	952w	ν(ring), $\rho(NH_2)$
		897w	843w	904w	ν(ring), $\rho(NH_2)$
816m			807m	800m	$\gamma(NH_2)$
792m		774w	784m	780m	ν(ring), δ(ring)
	760m	734m	760m	760m	ν(ring), δ(ring)
	732m	712m		731m	ν(ring), δ(ring)
700w	688w	696m		700m	NH_2 wagging
	647w				ν(ring), δ(ring)
601w		610w	599m	600m	ν(ring), δ(ring)
549m	568w	535w	579m	578m	NH_2 wagging
512m	518m		547w	544w	NH_2 wagging
	453w		431w	475w	NH_2 wagging

[a] Abbreviation: s, strong; m, medium; w, weak; br, broad; sh, shoulder; ν_{as}, asymmetric stretching; ν_s, symmetric stretching; δ, bending; ρ, libration, γ, out-of-plane bending.

3.3. Mass spectra

Mass spectroscopy is so useful that it can provide information about the relative molecular mass of a compound. Furthermore, it is frequently possible to determine which ligands or groups of atoms are bonded together from the way the compound breaks up or fragments during the experiment. Mass spectra of the bound complexes **1c** and **2c** appeared the molecular ion peak of the cationic species at $m/z = 400$ for $[Cu(L^1)(cyt)_2{-}H^+]^+$ and 490 for $[Cu(L^2)(cyt)_2{-}H^+]^+$, respectively. Furthermore, the fragment ions of a single cytosine-containing species, $[Cu(L^1)(cyt){-}H^+]^+$ and $[Cu(L^2)(cyt){-}H^+]^+$, were observed at $m/z = 289$ and 379, respectively. For **2c**, the m/z ratio at 268 has been assigned to the $[Cu(L^2){-}H^+]^+$ fragment. Finally, the protonated ligands $[(L^1)+2H^+]$ at 118 and $[(L^2)H]^+$ at 207 were also found. In the case of **1c**, the protonated cytosine species, $[(cyt)+H^+]$, was also found at $m/z = 112$. The obtaining results are therefore supported that two cytosine-bound complexes have been achieved. The possible fragmentation pathways for both complexes are schematically summarized as followed:

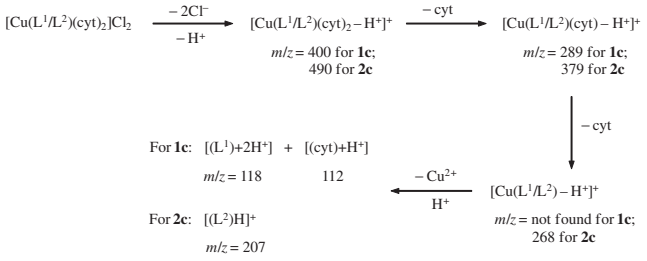

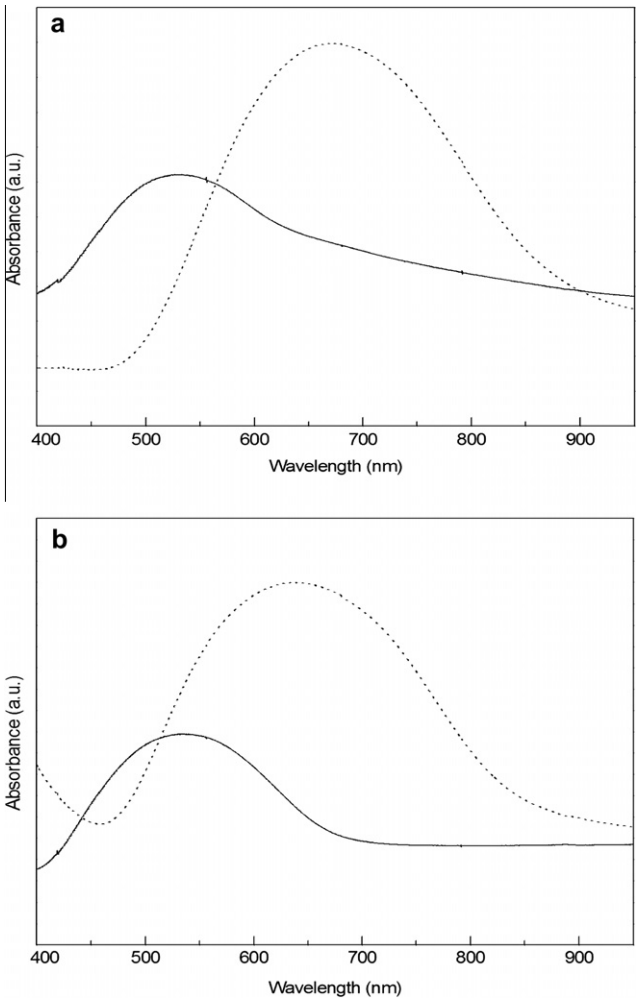

Fig. 2. Comparison of diffuse reflectance spectra of (a) complexes **1** (· · · ·) and **1c** (—) and (b) complexes **2** (· · · ·) and **2c** (—).

3.4. Diffuse reflectance spectra

Electronic spectra in solid state samples, obtained by diffuse reflectance spectrophotometry, are employed to ascertain the binding of complexes with the nitrogenous base cytosine. The covalent binding interaction between the copper(II) coordination compounds and cytosine DNA bases can be observed through the shifts in the d–d absorbance maxima of the copper(II) complexes in the visible range. The reflectance spectra of the free and bound complexes are shown in Fig. 2. Their maximum absorptions and their differences are collected in Table 2.

The copper(II) complexes **1** and **2** with blue in color showed a single broad d–d absorption band at $\lambda_{max} = 664.5$ nm (15 049 cm^{-1}) and 618.2 nm (16 176 cm^{-1}), respectively, indicative of approximate square pyramidal geometry [33]. In 1986, M.J. Begley et al. reported the copper(II) dimer of amidino-*O*-ethylurea (aOeu), $[Cu(aOeu)Cl_2]_2$ [34], which is rather similar to our systems. The $[Cu(aOeu)Cl_2]_2$ dimer appears as blue crystals with the absorption maxima at 670 nm (14 900 cm^{-1}) and reveals a square pyramid. According to these reports, it is supported that compounds **1** and **2** should possibly be a dimer and have been proposed to adopt a square pyramidal coordination with the formula of $[Cu(L^1)Cl_2]_2$ and $[Cu(L^2)Cl_2]_2$, respectively, as shown in Fig. 3.

Upon cytosine binding to the complexes **1** and **2**, the colors of solid products were changed to pink for **1c** and purple for **2c**, preliminarily suggesting that the bound complexes adopt the different coordination geometries and their copper centers have different environment from the initial complexes. Their reflectance spectra revealed that the d–d absorption peak of the bound complexes **1c** and **2c** showed the λ_{max} value of 517.4 nm (19 327 cm^{-1}) and 522.1 nm (19 153 cm^{-1}), respectively, recommending square-planar CuN_4 complexes [35–38]. Their maximum absorptions were significantly shifted to shorter wavelength

Table 2
Effect of cytosine on the electronic absorption bands and the EPR spectral parameters in a frozen DMSO solution at 77 K of the free complexes (**1** and **2**) and the bound complexes (**1c** and **2c**).

Complex	Color	Electronic spectral data, nm (cm^{-1})		EPR spectral data					
		λ_{max}	$\Delta\lambda_{max}$[a]	$g_{\|\|}$	$g_{\perp}$	G[b]	$A_{\|\|}$ (G)	$g_{\|\|}/A_{\|\|}$ (cm)	A_N (G)
1	Light blue	664.5 (15 049)	−147.1 (4278)	2.28	2.06	4.81	168	136	
1c	Pink	517.4 (19 327)		2.25	2.04	6.57	181	124	15
2	Deep blue	618.2 (16 175)	−96.1 (2978)	2.27	2.06	4.64	158	144	
2c	Purple	522.1 (19 153)		2.26	2.05	5.40	185	122	15

[a] $\Delta\lambda_{max} = \lambda_{bound} - \lambda_{free}$.
[b] $G = (g_{\|\|} - 2.0023)/(g_{\perp} - 2.0023)$.

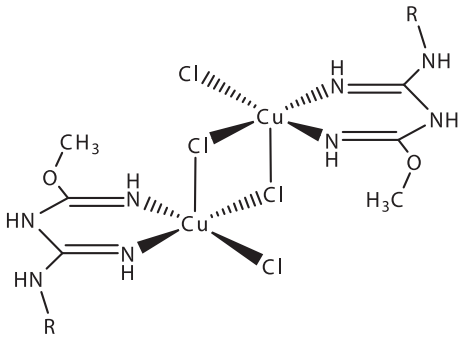

Fig. 3. Proposed structures of the free complexes **1** (R = H) and **2** ($R = CH_2C_6H_5$).

(hypsochromic or blue shift), thus resulting in the wavelength differences ($\Delta\lambda = \lambda_{bound} - \lambda_{free}$) of −147.1 nm (4278 cm^{-1}) and −96.1 nm (2978 cm^{-1}) (Table 2). The large shift is caused by coordination of cytosine to copper(II) center instead of the labile groups (Cl^-) in the initial complexes. This evidence helps us to further confirm the occurrence of the replacement of the two chloride ligands in **1** and **2** by two N(3)–cytosine molecules.

3.5. Electron spin resonance spectra

To gain further verification of the cytosine-binding ability of compounds **1** and **2**, EPR spectral studies was carried out in the frozen DMSO solution at 77 K. The spin Hamiltonian parameters provide the information on the stereochemistry of the copper(II) center and are significantly related to the type of donor atoms. Hence, this method can be utilized to monitor the interaction between copper(II) complexes and cytosine nucleobases. The X-band EPR spectra of the free and bound complexes are shown in Fig. 4. The EPR parameters are summarized in Table 2.

The obtained EPR spectra of all compounds are the typical anisotropic spectrum of monomeric copper(II) complexes where the four hyperfine lines in the $g_{||}$ region arising from the interaction of the $S = 1/2$ electron spin with the $I = 3/2$ copper nucleus are observed. The g tensor values are used to examine the electronic ground state of the copper center. The two initial and two bound complexes presented the trend of $g_{||} > g_{\perp} > 2.0$ and the G value higher than 4.0 suggesting that the unpaired electron of the copper(II) ion locates in the ground state $d_{x^2-y^2}$ orbital of an axial square-based geometry [39,40]. Noticeably, the minor signals at low field were observed in the spectra of the starting complexes (**1** and **2**), possibly due to the interaction between the complexes and solvent (DMSO) molecules.

EPR profiles of complexes **1c** and **2c** are considerably different from those of complexes **1** and **2** in the $g_{\perp}$ region. Nine superhyperfine splitting lines ($2nI_N + 1$) with the coupling value of 15 G found in the EPR spectra of **1c** and **2c** arise from four nitrogen donor atoms around the copper center. On the other hand, complexes **1** and **2** showed no nitrogen superhyperfine splitting in their spectra. This result is an important information to strongly confirm that the replacement of two chloride leaving groups in **1** and **2** by two nitrogen atoms from two cytosine molecules was occurred, thus resulting in changes of the chromophore from CuN_2Cl_2 (**1** and **2**) to CuN_4 (**1c** and **2c**). Additionally, a degree of distortion ($g_{||}/A_{||}$) can tell us the tetrahedral distortion of a square planar geometry and then the actual stereochemistry of the copper(II) complexes. The $g_{||}/A_{||}$ ratio in the range of 110–120 cm are typical for planar complexes, while the range of 130–150 cm is a characteristic of slight to moderate distortion and the range of 180–250 cm indicates considerable distortion [41,42]. The $g_{||}/A_{||}$ values of **1** and **2** are 136 and 144 cm, respectively, suggesting a slight to moderate distortion. The much lower values of the bound complexes of

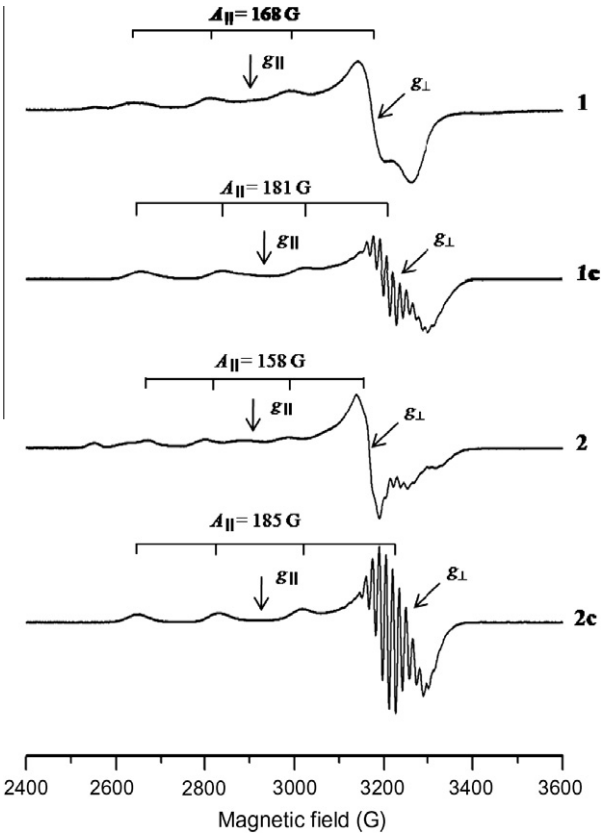

Fig. 4. X-band EPR spectra of a frozen DMSO solution of the starting complexes (**1** and **2**) and the cytosine-bound complexes (**1c** and **2c**) at 77 K.

124 cm for **1c** and 122 cm for **2c** appear to be nearly a typical planar complex.

The EPR results are strongly confirmed that cytosine nucleobases interact with complexes **1** and **2** through the substitution reaction of the N(3) cytosine atoms at the two chloride ligands in agreement with the large shift to higher energy in the electronic absorption bands in the bound complexes (**1c** and **2c**).

3.6. Thermal analysis

Thermogravimetric analysis is based on the change in mass of a sample as the temperature is varied, providing qualitative or quantitative information. Thermal decomposition processes of the bound complexes (**1c** and **2c**) are summarized in Table 3. Both complexes show the similar patterns with two steps of mass losses.

In the initial step of thermal decomposition of **1c** occurred in the temperature range from 50 to 450 °C which is attributed to the liberation of one chloride anion, the L^1 ligand and one cytosine molecule. An obvious weight loss of 54.8% (calc. 55.6%) appeared in this process with an endothermic peak at ~310 °C. An intermediate with proposed composition $[Cu(cyt)]Cl^+$ was formed. Its thermal decomposition in the last step between 450 and 1100 °C was the release of one remaining cytosine molecule with the found mass loss of 22.8% (calc. 23.5%) along with a sharp endothermic peak at 777 °C. Two steps of its thermal decomposition are demonstrated below:

$$[Cu(L^1)(cyt)_2]Cl_2 \xrightarrow[50\text{-}450^oC]{-\ L^1\ -\ cyt\ -\ Cl^-} [Cu(cyt)]Cl^+$$

$$[Cu(cyt)]Cl^+ \xrightarrow[450\text{-}1100^oC]{-\ cyt} CuCl^+$$

Table 3
Characteristic parameters of thermal decomposition for the cytosine bound complexes.

Complex	Step	Lost species	Decomp. range (°C)	DTA peak[a] (°C)	Weight loss (%)	
					Found	Calculated
$[Cu(L^1)(cyt)_2]Cl_2$, **1c**	1	$Cl^- + L^1 + cyt$	50–450	310	54.8	55.6
	2	cyt	450–1100	777	22.8	23.5
$[Cu(L^2)(cyt)_2]Cl_2$, **2c**	1	$2Cl^-$	60–230	148	12.1	12.6
	2	$L^2 + cyt$	230–425	296	56.2	56.4

[a] All showed endothermic peaks.

For **2c**, two steps of thermal decomposition appeared in the temperature range of 60–230 and 230–420 °C for the first and second processes, respectively. The first stage revealed the 12.1% loss of weight corresponding to the elimination of two chloride anions (calc. 12.6%) and confirming by an endothermic peak at 148 °C. The remaining species were proposed as $[Cu(L^2)(cyt)_2]^{2+}$. Then, the removal of the L^2 ligand and one cytosine molecule with the mass loss found 56.2% (calc. 56.4%) was manifested in the final disintegration stage corresponding to its DTA profile showing an endothermic peak at 296 °C. Two steps of its thermal decomposition are concluded as followed:

$$[Cu(L^2)(cyt)_2]Cl_2 \xrightarrow[60\text{-}230^oC]{-2Cl^-} [Cu(L^2)(cyt)_2]^{2+}$$

$$[Cu(L^2)(cyt)_2]^{2+} \xrightarrow[230\text{-}425^oC]{-L^2 - cyt} [Cu(cyt)]^{2+}$$

According to the thermal decomposition of both bound complexes, it is strongly recommended that two cytosine molecules can coordinate to the copper center by replacing the two chloride ligands of the complexes $[Cu(L^1/L^2)Cl_2]$ as desired.

3.7. Computational analysis

Due to the unsuccessful efforts to obtain suitable single crystals of **1c** and **2c** for structural analysis, molecular modeling studies were undertaken to gain a better understanding in the cytosine binding behavior and to investigate their coordination geometries.

The theoretical geometries for both compounds were calculated by the DFT method and optimized without restriction by using Dmol[3] module. Geometry optimizations were performed on two possible 4-coordinate conformers, square planar and tetrahedral forms, for the cationic species $[Cu(L^1)(cyt)_2]^{2+}$ and $[Cu(L^2)(cyt)_2]^{2+}$.

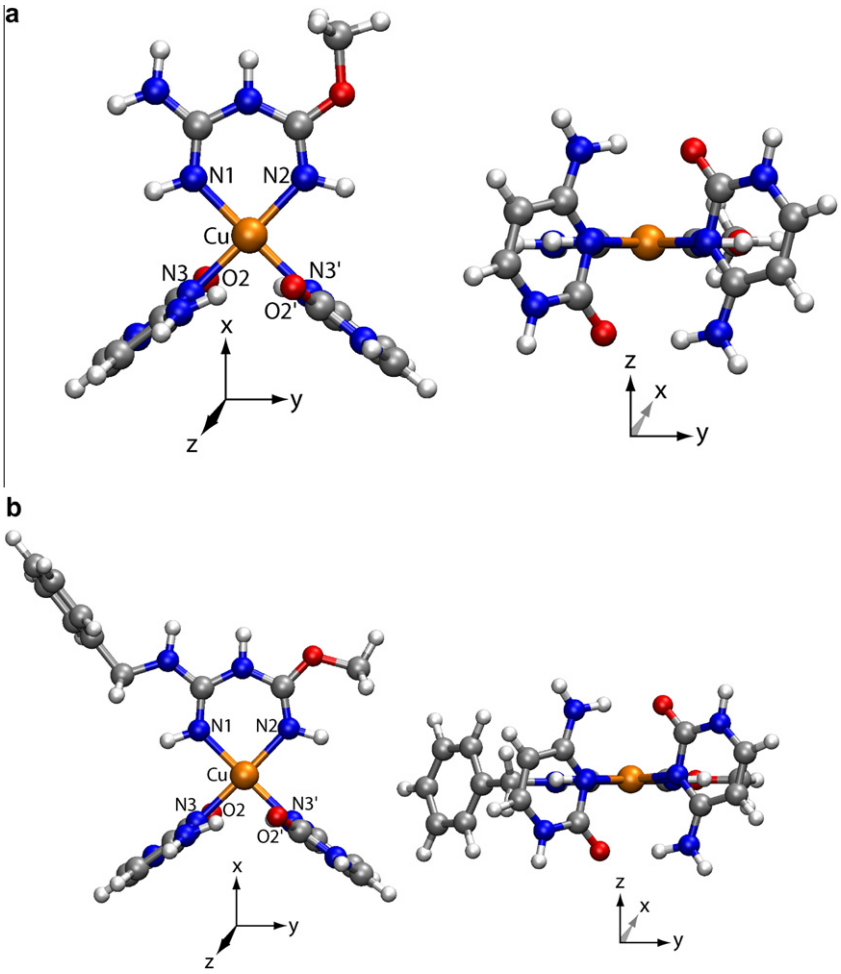

Fig. 5. Optimized geometries of (a) $[Cu(L^1)(cyt)_2]^{2+}$ and (b) $[Cu(L^2)(cyt)_2]^{2+}$ at the different views.

Each conformer was treated by placing the oxygen–O(2) atom of the two coordinated cytosine molecules in two orientations, at the same and opposite directions. Data of energy minimization for both conformers have shown that the strain energies of square planar structure are less than those of tetrahedral coordination in all cases. This result agrees well with the diffuse reflectance and EPR data of **1c** and **2c**. The optimized geometries are illustrated in Fig. 5 and the selected geometric parameters are collected in Table 4.

Table 4
Selected bond lengths (Å) and angles (°) for the optimized geometry of $[Cu(L^1)(cyt)_2]^{2+}$ and $[Cu(L^2)(cyt)_2]^{2+}$.

	$[Cu(L^1)(cyt)_2]^{2+}$	$[Cu(L^2)(cyt)_2]^{2+}$
Bond lengths		
Cu–N(1)	1.981	1.977
Cu–N(2)	1.978	1.997
Cu–N(3)	2.046	2.061
Cu–N(3′)	2.052	2.052
Bond angles		
N(1)–Cu–N(2)	88.1	88.3
N(3)–Cu–N(3′)	90.9	91.1
N(1)–Cu–N(3)	90.4	90.0
N(2)–Cu–N(3′)	90.6	90.6
N(1)–Cu–N(3′)	178.6	176.0
N(2)–Cu–N(3)	178.5	177.3

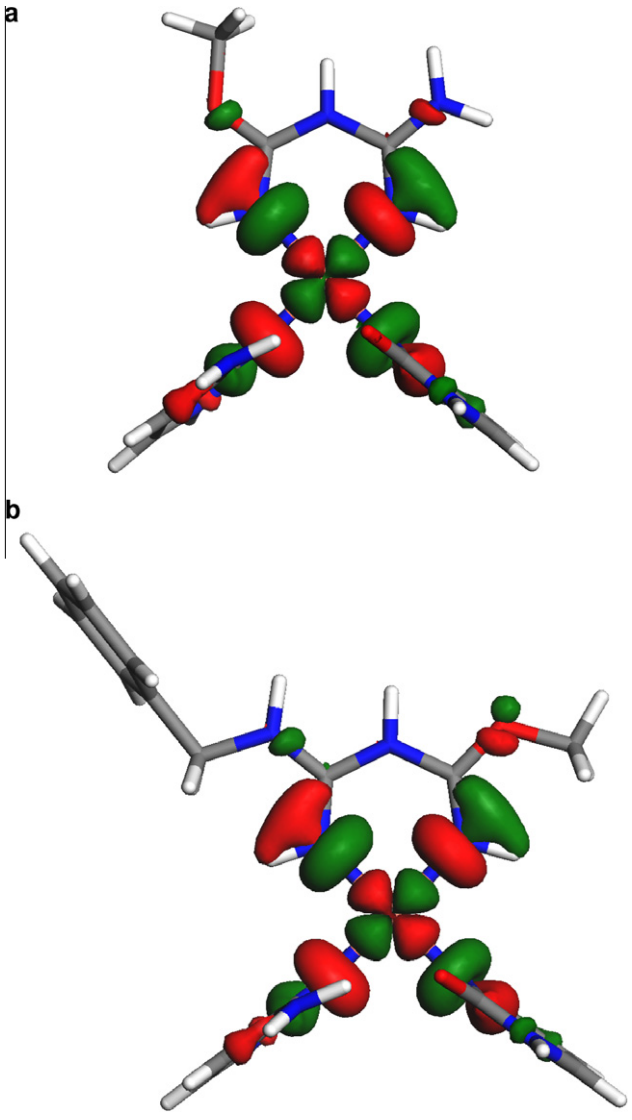

Fig. 6. Plots of the HOMOs for (a) $[Cu(L^1)(cyt)_2]^{2+}$ and (b) $[Cu(L^2)(cyt)_2]^{2+}$.

The optimized structure of $[Cu(L^1)(cyt)_2]^{2+}$ providing the lowest energy is a square planar coordination geometry where the O(2) atom of two cytosine molecules orientated in the opposite direction (Fig. 5a). The Cu–N bond lengths for Cu–L^1 and Cu–$(cyt)_2$ are ~1.98 and ~2.05 Å, respectively. In the case of $[Cu(L^2)(cyt)_2]^{2+}$, it was found the distortion in its optimized structure at the N(3) and N(3′) positions to be approximately 3° above and below the N(1)–Cu–N(2) plane (Fig. 5b). Therefore, the geometry optimization of $[Cu(L^2)(cyt)_2]^{2+}$ reveals a slightly distorted square planar with the two O(2)–cytosine atom in the opposite positions. Bond lengths between copper and nitrogen donors of L^2 and cytosine are in the range of 1.97–2.00 and 2.05–2.07 Å, respectively. Additionally, it is found that the Cu–O(2) and Cu–O(2′) distances are found to be the same length (2.78 Å) in compound **1c**. For compound **2c**, they are 2.82 and 2.81 Å, respectively. It is indicated that the two axial O(2)–cytosine atoms in both compounds are too far away to form coordinate covalent bonds with the copper center.

In order to investigate the binding interactions between cytosine bases and the present complexes, the total energy with zero-point vibrational energy (ZPVE) for each optimized structure was utilized to calculate the binding energy ($\Delta E_{binding}$). As the results, the ZPVE corrected energies of $[Cu(L^1)(cyt)_2]^{2+}$, $[Cu(L^2)(cyt)_2]^{2+}$, $[Cu(L^1)]^{2+}$, $[Cu(L^2)]^{2+}$ and cytosine are −894402.6, −1063985.9, −398684.8, −568298.7 and −247781.9 kcal/mol, respectively. The calculated $\Delta E_{binding}$ values are −154.0 and −123.4 kcal/mol for $[Cu(L^1)(cyt)_2]^{2+}$ and $[Cu(L^2)(cyt)_2]^{2+}$, respectively. These obtained binding energies have pointed that the two cytosine molecules are able to coordinate with the complex. The higher binding potential is found for $[Cu(L^1)(cyt)_2]^{2+}$. It can be clearly seen from a plot of the highest occupied molecular orbitals or HOMOs (Fig. 6) that the HOMOs of the cytosine-bound complexes are contributed by the orbitals from copper(II), ligand and cytosine, strongly confirming the occurrence of the cytosine-binding to the complex.

4. Conclusions

Copper(II) chloride complexes of *N*,*N*-bidentate L^1 and L^2 ligands were prepared and studied on their cytosine-binding abilities. Interactions of complexes **1** and **2** with two cytosine bases were investigated by several basic techniques. Results exhibit a strong evidence to confirm the capability of both complexes to coordinate with two N(3)–cytosine molecules by replacing two chloride ligands, yielding the bifunctional adducts **1c** and **2c**. The theoretical calculations have shown their optimized structures as a square planar geometry. The ~20% lower binding energy for **1c** than **2c** indicates the stronger binding potential to cytosine. The reason may arise from the fact that compounds **1** and **2** contain the different *N*-substitution groups on the ligand, NH_2 and $NHCH_2(C_6H_5)$, respectively. The phenyl moiety could be possible to sterically interfere the incoming cytosines to replace the chlorides on the opposite site. However, this factor would be a little impact on the coordination geometry. Therefore, the optimized structure of **2c** tends to be slightly distorted from the perfect square planar geometry, while that of **1c** is a square planar. Here we have shown that copper(II) complexes with bidentate ligands like the L^1 and L^2 ligands are good candidates for binding to cytosines and worthwhile further developing to be a DNA-binding agent.

Acknowledgments

The authors are grateful to the Center of Excellence for Innovation in Chemistry (PERCH-CIC), Khon Kaen University, the

Development and Promotion of Science and Technology Talents Project (to A.M.), and the Office of the Higher Education Commission under National Research University Project for their financial support. The computer resource was supported by the National Nanotechnology Center (NANOTECH).

References

[1] A. Eastman, in: B. Lippert (Ed.), Cisplatin: Chemistry and Biochemistry of a Leading Anticancer Drug, VHCA and Wiley-VCH, Zurich and Germany, 1999, p. 111.
[2] T.W. Hambley, J. Chem. Soc., Dalton Trans. (2001) 2711.
[3] H.M. Pinedo, J.H. Schornagel (Eds.), Platinum and Other Metal Co-ordination Compounds in Cancer Chemotherapy, vol. 2, Plenum, New York, 1996.
[4] M.J. Bloemink, H. Engelking, S. Karentzopoulos, B. Krebs, J. Reedijk, Inorg. Chem. 35 (1996) 619.
[5] J.A. Navarro, J.M. Salas, M.A. Romero, R. Vilaplana, F. Gonzalez-Vilchex, R. Faure, J. Med. Chem. 41 (1998) 332.
[6] M.P.M. Marques, T. Girao, M.C. Pedroso de Lima, A. Gameiro, E. Pereira, P. Garcia, Biochim. Biophys. Acta 1589 (2002) 63.
[7] Y. Jung, S.J. Lippard, Chem. Rev. 107 (2007) 1387.
[8] I. Eryazici, C.N. Moorefield, G.R. Newkome, Chem. Rev. 108 (2008) 1834.
[9] M.C. Linder, M. Hazeqh-Azam, Am. J. Clin. Nutr. 63 (1996) 797s.
[10] F. Saczewski, E. Dziemidowicz-Borys, P.J. Bednarski, R. Grunert, M. Gdaniec, P. Tabin, J. Inorg. Biochem. 100 (2006) 1389.
[11] J. He, P. Hu, Y.-J. Wang, M.-L. Tong, H. Sun, Z.-W. Mao, L.-N. Ji, Dalton Trans. (2008) 3207.
[12] C.M. Mikulski, C.J. Lee, T.B. Tran, Inorg. Chim. Acta 136 (1987) L13.
[13] D. Tran Qui, E. Palacios, Acta Crystallogr., Sect. C 46 (1990) 1220.
[14] G. De Munno, S. Mauro, T. Pizzino, D. Viterbo, J. Chem. Soc., Dalton Trans. (1993) 1113.
[15] A. Panfil, A. Terrón, J.J. Fiol, M. Quiros, Polyhedron 13 (1994) 2513.
[16] M. Palaniandavar, I. Somasundaram, M. Lakshminarayanan, H. Manohar, J. Chem. Soc., Dalton Trans. (1996) 1333.
[17] G. De Munno, M. Medaglia, D. Armentano, J. Anastassopoulou, T. Theophanides, J. Chem. Soc., Dalton Trans. (2000) 1625.
[18] P.T. Selvi, M. Murali, M. Palaniandavar, M. Kockerling, G. Henkel, Inorg. Chim. Acta 340 (2002) 139.
[19] S. Kalyanaraman, V. Krishnakumar, K. Ganesan, Spectrochim. Acta 66A (2007) 1340.
[20] P.M. van Vliet, J.G. Haasnoot, J. Reedijk, Inorg. Chem. 33 (1994) 1934.
[21] A.C.G. Hotze, A.H. Velders, F. Ugozzoli, M.B. Cingi, A.M.M. Lanfredi, J.G. Haasnoot, J. Reedijk, Inorg. Chem. 39 (2000) 3838.
[22] U. Suksangpanya, A.J. Blake, P. Hubberstey, D.J. Parker, S.J. Teat, C.L. Wilson, CrystEngComm 5 (2003) 10.
[23] O. Jardetzsky, P. Pappas, N.G. Wade, J. Am. Chem. Soc. 85 (1963) 1657.
[24] M. Sundralingam, J.A. Carrabine, J. Mol. Biol. 61 (1971) 287.
[25] S. Shirotake, T. Sakaguchi, Chem. Pharm. Bull. 25 (1977) 3232.
[26] D.J. Szalda, L.G. Marzilli, T.J. Kistenmacher, Inorg. Chem. 14 (1975) 2076.
[27] U. Chaveerach, A. Meenongwa, Y. Trongpanich, C. Soikum, P. Chaveerach, Polyhedron 29 (2010) 731.
[28] Material Studio 4.3, Accelrys Software Inc., San Diego, CA, 2008.
[29] B. Delley, Phys. Rev. B. 66 (2002) 155125/1.
[30] P. Tyagi, P. Gahlot, R. Kakkar, Polyhedron 27 (2008) 3567.
[31] R. Kakkar, R. Grover, P. Gahlot, Polyhedron 25 (2006) 759.
[32] R. Wagner, W. von Philipsborn, Helv. Chim. Acta 53 (1970) 299.
[33] A.B.P. Lever, Inorganic Electronic Spectroscopy, Elsevier, New York, 1984.
[34] M.J. Begley, P. Hubberstey, C.H.M. Moore, J. Chem. Res. (S) (1986) 172.
[35] L. Fabbrizzi, P. Paoletti, A.B.P. Lever, Inorg. Chem. 15 (1976) 1502.
[36] A.W. Addison, M. Carpenter, L.K.M. Lau, M. Wicholas, Inorg. Chem. 17 (1978) 1545.
[37] A.W. Addison, M. Palaniandavar, W.L. Driessen, F. Paap, J. Reedijk, Inorg. Chim. Acta 142 (1988) 95.
[38] T. Pandiyan, M. Palaniandavar, M. Lakshminarayanan, H. Manohar, J. Chem. Soc., Dalton Trans. (1992) 3377.
[39] I.M. Procter, B.J. Hathaway, P. Nicholas, J. Chem. Soc., Section A (1968) 1678.
[40] B.J. Hathaway, D.E. Billing, Coord. Chem. Rev. 5 (1970) 143.
[41] A.W. Addison, Spectroscopic and redox trends from model copper complexes, in: K.D. Karlin, J. Zubieta (Eds.), Copper Coordination Chemistry: Biological and Inorganic Perspectives, Adenine Press, New York, 1983.
[42] V.V. Pavlischuk, Theor. Exp. Chem. 31 (1995) 1.